Journal of Catalysis **197,** 281–291 (2001)
doi:10.1006/jcat.2000.3097, available online at http://www.idealibrary.com on IDEAL®

Mechanism of the Selective Reduction of NO_x over Co/MFI: Comparison with Fe/MFI

Xiang Wang, Hai-Ying Chen, and Wolfgang M. H. Sachtler

V. N. Ipatieff Laboratory, Center for Catalysis and Surface Science, Department of Chemistry, Northwestern University, Evanston, Illinois 60208

Received May 31, 2000; revised October 23, 2000; accepted October 23, 2000; published online December 21, 2000

Co/MFI and Fe/MFI have been compared in catalytic tests of NO_x reduction with isobutane and methane. FTIR, TPD-MS, and MS data of catalytic results with labeled molecules reveal a similar multistep mechanism over both catalysts for reduction with isobutane, but NO_x reduction with methane over Co/MFI is qualitatively different. Reactive NO_y (nitro and nitrate) groups are assumed to be formed from NO and an adsorbed superoxide ion, which was identified by its EPR signal at 77 K. Formation of nitrate ions and NO_2 ligands is easily explained with this model. With isobutane as the reductant, Fe/MFI is more active, but Co/MFI is more selective, leading to 100% N_2 yield. The primary intermediate is a deposit, exposing nitrile and isocyanate groups; the latter react with NO_x to form N_2 with one N atom from the deposit and the other from NO. An important difference between Co/MFI and Fe/MFI is the formation of zerovalent metal clusters in the former case and its absence in the latter. Clusters of Co_n^0 have been detected by EPR in catalysts with high Co loading after reduction at 300°C. They catalyze the H/D exchange of CH_4 with D_2. The possibility is discussed that under certain conditions such clusters could contribute to the activation of methane.

Key Words: **NO_x reduction with hydrocarbons; Co/MFI or Co/ZSM-5 catalysts for NO_x reduction; Fe/MFI or Fe/ZSM-5 catalysts for NO_x reduction; O_2 adsorption as superoxide ion; metal/zeolite preparation by sublimation; mechanism of NO_x reduction over zeolite-based catalysts; cobalt oxo ions; reduction of Fe^{3+}/Fe^{2+} versus Co^{2+}/Co^0 redox couples in zeolites.**

1. INTRODUCTION

For the reduction of NO_x (any mixture of NO and NO_2) with hydrocarbons in emissions containing a large excess (with respect to NO_x) of oxygen and steam, two catalysts carry considerable promise:

1. Fe/MFI with high Fe loadings corresponding to Fe/Al ∼ 1, where Al stands for the number of Al centered tetrahedra in the MFI (also called ZSM-5) zeolite (1–6). Such catalysts have been obtained by a procedure in which sublimation of $FeCl_3$ vapor onto the H form of the zeolite is an important step. NO_x is reduced to N_2 by i-C_4H_{10} in gas streams with a GHSV of 42,000 h^{-1}. N_2 yields exceeding 70% are achieved at a temperature near 350°C.

2. Co/MFI prepared by a variety of techniques (7, 8). Among these preparations, two lead to promising catalysts: (a) wet ion exchange, resulting in materials with Co/Al ratios of typically 0.45; (b) sublimation of a volatile Co halide onto H-MFI, resulting in materials with a Co/Al ratio ∼ 1. With i-C_4H_{10} as the reductant, N_2 yields of ∼100% have been achieved over both types of Co/MFI catalysts, but with the class (b) materials this yield is reached at a ∼50°C lower temperature than with those of class (a).

In previous papers, extensive characterizations of the Fe/MFI catalysts have been described and models have been proposed on the active sites (1–6, 9–19). Crucial steps in NO_x reduction with light alkanes have been identified. As Co and Fe are neighbors in the periodic table, it is tempting to assume that the same models should also be applicable to Co/MFI catalysts. There are, however, some significant differences that show that great caution is needed before models that are based on data obtained with Fe/MFI should be applied to the Co/MFI catalysts. Two differences are of possible significance:

1. Whereas Fe/MFI is unable to catalyze NO_x reduction with methane (3), Co/MFI catalysts display remarkable activity for this reaction, at least in the absence of water (8, 20, 21). N_2 yields near 35% have been obtained.

2. TPR data show that, in the temperature range of high activity for selective NO_x reduction, the iron in Fe/MFI is reversibly reduced from Fe^{3+} to Fe^{2+} (1), but the cobalt in Co/MFI is reduced to Co^0 (7). The reduction of an isolated Co^{2+} ion to an isolated Co^0 atom will, of course, be highly endothermic in comparison to the reduction of a multinuclear oxo ion or oxide particle to a multiatomic Co_n^0 cluster, the energy difference being of the order of the heat of sublimation (∼100 kcal/mol). This explains the observation that the reduction of Co^{2+} ions in Co/MFI prepared by ion exchange from aqueous solution requires a high temperature of ∼700°C and still remains incomplete. In contrast, catalysts that are prepared by impregnation or sublimation contain Co_3O_4 particles or multinuclear oxo ions, which are completely reduced at a much lower temperature. As NO_x reduction with a hydrocarbon is, of course, a catalyzed oxidation of the latter, one should keep in mind

0021-9517/01 $35.00

that Co/MFI appears to be an oxidation catalyst based on the $\boldsymbol{n}\mathbf{Co}^{2+}/\mathbf{Co}_{\boldsymbol{n}}^{0}$ redox couple, whereas Fe/MFI apparently uses the $\mathbf{Fe}^{3+}/\mathbf{Fe}^{2+}$ couple.

In the present work Fe/MFI and Co/MFI catalysts have been compared experimentally. TPD-MS and FTIR have been used to identify adsorption complexes and stable intermediates. A circulation system equipped with a mass spectrometer has been applied to monitor the gas phase products of NO_x reduction with hydrocarbons. CH_4 exchange with D_2 over a partially reduced Co/MFI-SUB catalyst was used as a probe for the presence of Co^0 clusters in the reduced catalyst.

2. EXPERIMENTAL

2.1. Catalyst Preparation

Fe/MFI was prepared by first subliming $FeCl_3$ vapor onto the H-form of an MFI zeolite at 320°C, followed by treatment with doubly deionized water (1). Such catalysts will be called Fe/MFI-SUB. Co/MFI catalysts were prepared by two methods: (1) Co/MFI-WIE is obtained by traditional wet ion exchange between H-MFI and a diluted $CoCl_2$ solution (7); (2) Co/MFI-SUB is prepared by first subliming $CoCl_2$ (Aldrich, >98%) or $CoBr_2$ (Aldrich, 99%) vapor onto the H-form of MFI zeolite; the detailed procedure is described elsewhere (7, 8). The H-MFI precursor was obtained by three-fold ion exchange of Na/MFI (Si/Al = 14.0, Na/Al = 0.73, Degussa) with a diluted NH_4NO_3 solution to the NH_4^+ form at ambient temperature, followed by calcination in a UHP O_2 flow at 550°C for 4 h.

In the preparations using sublimation, $FeCl_3$ or Co halide vapor diffuses into the H-form MFI zeolite channels, where they react with zeolite protons,

$$H^+ + FeCl_3 = [FeCl_2]^+ + HCl\uparrow \qquad [1]$$

$$H^+ + CoX_2 = [CoX]^+ + HX\uparrow, \qquad [2]$$

until virtually all protons are replaced, thus leading to samples with Fe/Al or Co/Al ∼ 1. After this procedure Fe and Co samples were hydrolyzed and washed with doubly deionized water to remove halides. In this step, a small concentration of Brønsted acid sites is regenerated (1, 7). After drying in air at ambient temperature, the samples were calcined in a UHP oxygen flow at 550°C for 4 h.

Elemental analysis via inductively coupled plasma spectroscopy (ICP) gives the following compositions relative to Al:

Fe/MFI-SUB: Fe/Al = 1.0, Si/Al = 14.0, Na/Al = 0.

Co/MFI-WIE: Co/Al = 0.44, Si/Al = 14.0, Na/Al = 0.

Co/MFI-SUB: Co/Al = 1.13, Si/Al = 14.0, Na/Al = 0.

2.2. Catalytic Tests

These were carried out in a U-shaped fixed-bed microreactor with continuous downflow at a constant pressure of 1 bar, while the temperature was increased in a programmed manner. Typically, 0.2 g of catalyst powder was used. Before the tests, the catalysts were stabilized at 400°C overnight in the dry feed, followed by recalcination in 10% O_2 at 500°C for 1 h. For the reduction of NO_x with i-C_4H_{10}, a typical feed was 0.2% NO, and 0.2% i-C_4H_{10}, 3% O2, balanced with He. The total flow rate was 280 ml/min. Based on a bulk density of 0.5 g/ml of the zeolite, the calculated GHSV was 42,000 h^{-1}. For the tests with CH_4, the conditions were chosen similar to those employed by Li and Armor (21, 22), i.e., the inlet gas compositions were 0.16% NO, 0.1% CH_4, and 2.5% O_2, balanced by He with a total flow rate of 200 ml/min, which corresponds to a GHSV of 30,000 h^{-1}. When desired, 10% H_2O was added to either feed using an H_2O saturator. To avoid water condensation, the feed line was heated with heating tapes. Data were collected at constant temperature of the catalyst, after preconditioning it for 30 min at each temperature. Between these preset temperatures, a ramp of 8°C/min was used and data were collected at ascending temperature. The NO conversion was calculated from the measured values of the formed N_2. The hydrocarbon conversion was calculated from the amount of CO_2 and CO in the effluent.

2.3. NO, NO + O_2 Adsorption and Temperature-Programmed Desorption Studies

The measurements were carried out on a TPD-MS system with a quartz reactor loaded with 0.2 g of sample on a porous frit. The samples were first calcined in a 60 ml/min UHP O_2 flow at 600°C for 1 h, followed by cooling to ambient temperature in the same flow. Subsequently, the samples were purged with a 60 ml/min UHP He flow for 30 min. Adsorption was measured with a mixture of NO (0.5%) in He (for NO only) or NO (0.5%) + O_2 (3%) in He (for NO + O_2) at a flow rate of 60 ml/min. The gas mixture flow first bypassed the catalyst to get a background signal and then passed through the catalyst bed at room temperature. The changes in the MS signal intensity were monitored during the adsorption. Once equilibrium was established again, the gas flow was switched back to the 60 ml/min UHP He flow and the catalyst was purged for ∼1 h. A TPD profile was then recorded in the same He flow while the temperature was increased from room temperature to 600°C with a ramp of 8°C/min.

2.4. FTIR Spectroscopy

Infrared spectra were collected with a Nicolet 60SX FTIR spectrometer, equipped with a liquid N_2 cooled mercury cadmium telluride (MCT) detector. Each sample was pressed into a self-supporting wafer with a diameter of

13 mm and a mass of 10 mg. The wafer was inserted into a quartz cell sealed with NaCl windows connected to the gas manifold. The sample was calcined *in situ* at 450°C in a 50 ml/min O_2/He (10%) flow for 1 h and then cooled to 200°C in the same flow. In the following experiments the temperature was held at 200°C. For NO adsorption, a 100 ml/min gas mixture of NO (0.5%) + He was passed through the cell for 30 min, followed by purging with a 100 ml/min flow of UHP He or O_2(2.5%) + He for 40 min. For NO + O_2 adsorption, a gas mixture of NO (0.5%) + O_2 (2.5%) + He at 100 ml/min was passed through the cell for 60 min, followed by purging with O_2 (2.5%) + He at 100 ml/min for 60 min. To investigate the reactivity of the adsorbed species, a gas mixture of *i*-C_4H_{10} or CH_4 (0.25%) + O_2 (2.5%) + He was introduced into the cell. All spectra were taken at constant temperature, accumulating 64 scans with a spectral resolution of 1 cm^{-1}. The gas inside the cell immediately after scanning of a sample was used as the spectroscopic background. In this paper, the spectrum of the calcined sample was always subtracted from that of the sample covered with adsorbate, both spectra being collected under flow conditions.

2.5. *Mass Spectrometric Analysis*

A recirculating manifold equipped with a Dycor quadrupole gas analyzer was used to analyze the released gases. A 0.15-g Co/MFI-WIE or Co/MFI-SUB catalyst was loaded into a Pyrex reactor, which was attached to the system. Prior to the experiment, the catalyst was calcined in a 100 ml/min UHP O_2 flow at 500°C for 1 h and cooled to 200°C. With the catalyst held at this temperature, the system was pumped (background pressure, 10^{-3} Torr) for 0.5 h before a known amount of gas was admitted to the sample loop and circulated over the catalyst. Signal intensities were normalized by using the Ar^{2+} peak ($m/e = 20$) as an internal standard.

2.6. *CH_4 Exchange with D_2 over Partially Reduced Co/MFI-SUB*

A recirculating manifold equipped with a Dycor quadrupole gas analyzer was used.

A 0.2-g Co/MFI-SUB catalyst prepared from $CoCl_2$ was loaded into a Pyrex reactor, which can be attached to the system. Prior to the H/D exchange, the sample was reduced in an H_2/Ar (5%) flow, with the temperature increasing from 23 to 300°C with a ramp of 8°C/min, followed by a constant temperature of 300°C for 1 h. Previous TPR results revealed a low-temperature peak below 300°C (7); this Co species should be reduced to Co^0 by the described procedure. Our unpublished EPR data show that Co^0 clusters are formed by it.

After the temperature was lowered to 25°C in the same H_2/Ar flow, the gas was replaced by flowing Ar for 30 min. The reactor with the reduced sample was then sealed and transferred to the recirculating system. To exclude any reaction between D_2 and residual oxygen species, the sample was re-reduced with 80 Torr D_2 at 300°C for 1 h in the circulation system, followed by evacuation for 30 min. Subsequently, a mixture of 40 Torr CH_4 (Matheson, UHP) and 40 Torr D_2 (Linde, CP) was introduced into the system. Both gases had been purified over MnO and a 5A molecule sieve trap to remove undesired traces of O_2 or H_2O. The D_2 had been held over an additional liquid N_2 trap for further purification.

3. RESULTS

3.1. *Comparison of the Catalytic Performance in NO_x Reduction*

The catalysts Fe/MFI-SUB, Co/MFI-WIE, and Co/MFI-SUB were tested under standard conditions with either *i*-C_4H_{10} or CH_4. In Fig. 1, the N_2 yields are plotted against the reaction temperature. With *i*-C_4H_{10} as the reductant (Fig. 1a), Fe/MFI-SUB is the most active catalyst below 350°C and a maximum N_2 yield of 76% is obtained. Above this temperature, the N_2 yield decreases, becoming ~30% at 500°C. Apparently, the reaction of *i*-C_4H_{10} with O_2 competes successfully against its reaction with NO_x at high temperature. However, over the Co/MFI catalysts the N_2 yield continues to increase until 100% is approached. This yield is reached at a ~50°C lower temperature over Co/MFI-SUB than over Co/MFI-WIE. The N_2 yield thus remains higher over Co/MFI-SUB up to 450°C. The Co content of this catalyst is about twice that of Co/MFI-WIE; our previous work has shown that Co/MFI-SUB contains appreciable amounts of Co_3O_4 and Co oxo ions, whereas in Co/MFI-WIE only isolated Co ions are detected, which are reducible only at very high temperature (7, 8). Unlike Fe/MFI-SUB, the two Co/MFI catalysts maintain high N_2 yields > 80% at temperatures above 400°C. All three catalysts show remarkable hydrothermal stability with *i*-C_4H_{10} as the reductant;

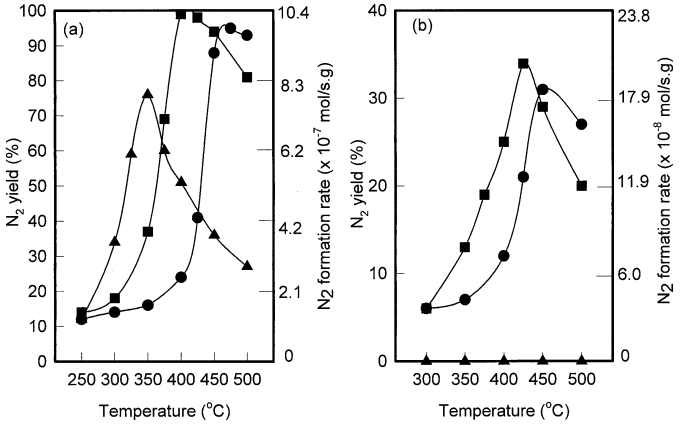

FIG. 1. Selective reduction of NO_x with (a) *i*-C_4H_{10} and (b) CH_4 over Fe/MFI and Co/MFI catalysts in dry feed.

the catalytic performance is not impaired in the presence of 10% water vapor (1, 7, 8).

With CH_4 (Fig. 1b), Fe/MFI-SUB shows no measurable activity for NO_x reduction in the whole temperature region, but both Co/MFI catalysts show substantial activity, the maximum N_2 yield being ~30%. Again, Co/MFI-SUB is more active than Co/MFI-WIE below 450°C, and in this temperature region Co/MFI-SUB reaches a given N_2 yield at a ~50°C lower temperature than Co/MFI-WIE.

3.2. *NO, NO + O_2 Adsorption and Desorption*

To clarify the effect of O_2 on the catalytic activity, the adsorption of NO and mixtures of NO + O_2 was studied and subsequent temperature-programmed desorption was monitored by mass spectrometry. When an NO + O_2 feed was used, a very small $m/e = 46$ signal was observed, even when the catalyst was bypassed, indicating some reaction of NO with O_2 in the gas phase or on the metal walls of the ducts.

NO is adsorbed by exposing the Co/MFI catalysts to a flow of NO (0.5%) + He and saturation is reached at ~20 min. The adsorption rate is much lower than with Fe/MFI under similar conditions (3). After being purged in flowing UHP He at room temperature for ~30 min, the adsorbate is characterized. The TPD profiles are shown in Fig. 2. With both catalysts NO desorption ($m/e = 30$) is evident below 300°C. A small O_2 peak ($m/e = 32$), which appears at higher temperature, in concert with a second $m/e = 30$ signal is possibly caused by decomposition of some NO_y complexes that might have been formed either from an NO_2 impurity or by reaction of NO with residual oxygen in the system.

It takes longer for NO + O_2 to give constant gas phase signals than for pure NO. This rate depends on the nature of the catalyst. Over Co/MFI-WIE, the NO + O_2 mixture reaches a constant composition after ~100 min, whereas

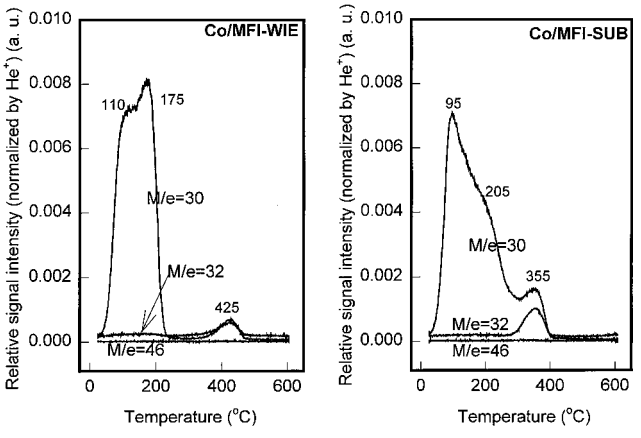

FIG. 2. TPD profiles of Co/MFI-WIE and Co/MFI-SUB samples after exposure to a NO (0.5%) + He flow and purge with a He flow at room temperature.

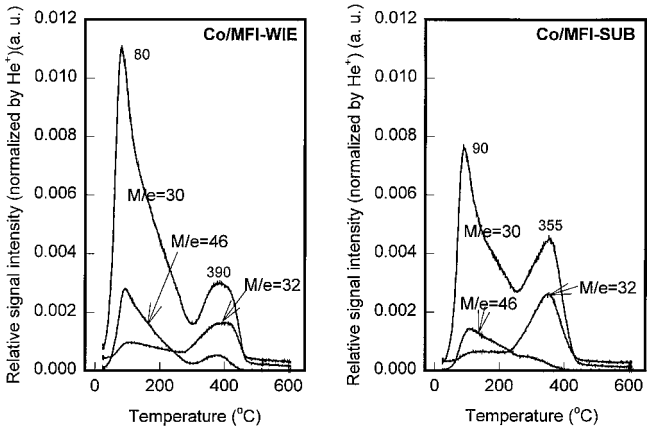

FIG. 3. TPD profiles of Co/MFI-WIE and Co/MFI-SUB samples after exposure to a NO (0.5%) + O_2 (3%) + He flow and purge with a He flow at room temperature.

over Co/MFI-SUB it takes only ~65 min. With either Co/MFI catalyst, this rate is significantly lower than that with Fe/MFI-SUB (3).

TPD profiles of the catalysts following exposure to NO + O_2 are shown in Fig. 3. The main difference with the TPD profiles in Fig. 2 is the appearance of NO_2, which is identified by its parent peak at $m/e = 46$ and a satellite at $m/e = 30$. At low temperature this satellite is mainly caused by fragmentation of NO_2 inside the ionization chamber of the mass spectrometer; the ratio of both peaks does not deviate substantially from the value of 2.7 given in Ref. (23) for a different instrument. Of greater interest are the peaks at higher temperature (390°C for the WIE and 355°C for the SUB sample) The $m/e = 30$ peak then appears in concert with an O_2 peak at $m/e = 32$, indicating thermal dissociation of an adsorbed NO_y complex. The data confirm that NO_y chemisorption complexes are formed in the presence of NO + O_2.

3.3. *FTIR Identification of Adsorption Complexes and Deposits*

3.3.1. NO adsorption. Since the two Co/MFI samples show similar FTIR spectra, only those of Co/MFI-SUB are shown in Fig. 4. After the catalyst wafer was exposed to an NO (0.5%) + He flow at 200°C for 30 min, adsorption reached saturation. Four bands are observed at 2131, 1804, 1885, and 1933 cm^{-1}. The band at 2131 cm^{-1} has been assigned to NO^+ on Brønsted acid sites in the zeolite (24). Its intensity is very weak, in line with our previous result that the concentration of Brønsted acid sites in Co/MFI-SUB is very low (7, 8). On Co/MFI-WIE this band is a little stronger. The 1804- and 1885-cm^{-1} bands have been assigned to the asymmetric and symmetric N–O stretching vibrations of the dinitrosyl complex $Co^{2+}(NO)_2$ (25–30). The band at 1940 cm^{-1} is assigned to mononitrosyl groups on Co^{2+} (24–29) or Co^{3+} (30). After the samples were purged

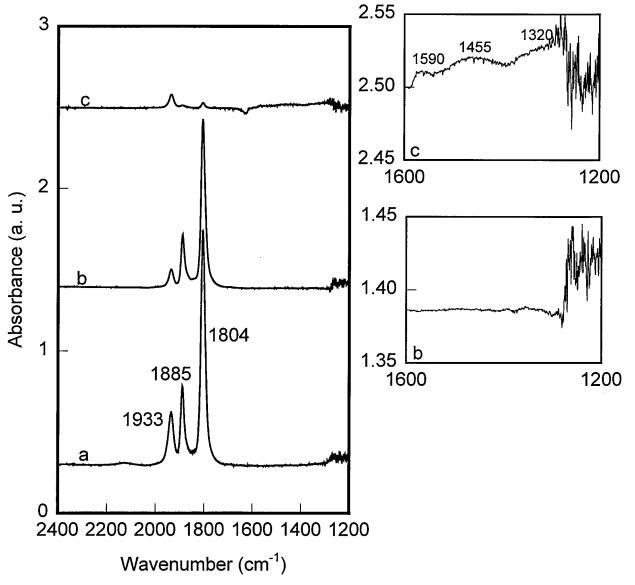

FIG. 4. FTIR spectra taken at 200°C of Co/MFI-SUB after (a) NO (0.5%) + He adsorption for 30 min, (b) subsequently purged by a He flow for 40 min, or (c) purged by a O_2 (2.5%) + He flow for 40 min.

with UHP He flow for 40 min, the intensity of the dinitrosyl and the mononitrosyl bands decreased by ~30 and ~70%, respectively, without formation of new bands, indicating thermal desorption of the NO groups. However, a different result is observed upon purging with an O_2 (2.5%) + He flow for 40 min. The dinitrosyl bands almost disappear, and the mononitrosyl band decreases by 80%. In the region of 1200–1600 cm^{-1} (see the enlarged Fig. 4c), new bands of low intensity emerge, which are assigned to NO_y complexes. In summary, the NO adsorbates react with O_2 and are converted to NO_y groups (27, 31).

3.3.2. $NO + O_2$ adsorption. The FTIR spectra of $NO + O_2$ on Co/MFI-SUB are shown in Fig. 5. The same bands due to NO^+, Co^{2+}–NO, and $Co^{2+}(NO)_2$ are observed as in Fig. 4. The intensity of the mononitrosyl band is similar to that in Fig. 4, while the intensity of the dinitrosyl bands is much weaker. The NO^+ band is stronger since NO^+ is proposed to occur via the following equilibrium:

$$2NO + \tfrac{1}{2}O_2 + 2H^+ \rightleftarrows H_2O + 2NO^+. \qquad [3]$$

In addition to the four bands belonging to NO adsorbates, new overlapping bands emerge at 1320, 1455, 1571, and 1590 cm^{-1}. Similar bands have been reported by others, but there is incomplete agreement on the assignment (25, 27, 30, 32, 33). In view of our TPD results, we assign them to NO_2 or nitrate groups, i.e., the NO_y complexes.

As the spectra a–c in Fig. 5 show, these bands appear rapidly in the first 10 min upon exposure to $NO + O_2$; thereafter, they slowly increase further. With Co/MFI-SUB, it takes ~60 min to reach saturation; but with Co/MFI-WIE, it takes ~80 min. This is in line with the mentioned changes in the gas phase during the $NO + O_2$ adsorption. Curves d–f in Fig. 5 show the stability of the adsorption bands in O_2 + He flow at 200°C. Upon the samples being purged for 30 min, the bands corresponding to NO^+ and $Co^{2+}(NO)_2$ disappear completely, while the small band of Co^{2+}–NO survives. In contrast, the bands of the NO_y complexes at 1590 and 1571 cm^{-1} do not decrease during purging, but in fact become even stronger. This indicates that not only are the NO_y complexes thermally stable at 200°C in flowing O_2 + He but also even more NO_y is formed. These data thus indicate that nitrosyl groups on Co^{2+} sites can be oxidized by O_2 to NO_y complexes (27, 31).

3.3.3. Reactivity of NO_y complexes with i-C_4H_{10} and CH_4. The spectra in Fig. 6 show the reactivity of the thermally stable NO_y complexes toward *i*-C_4H_{10} at 200°C. Upon exposure to a flow of *i*-C_4H_{10} (0.25%) + O_2 (2.5%) + He, the NO_y bands at 1590 and 1320 cm^{-1} vanish very quickly. After 10 min, new bands at 1376, 1426, 1662, 2175, 2202, 2260, 2317, 2955, and 3157 cm^{-1} are observed. Their intensity increases with exposure time, reaching saturation after ~60 min.

As Fig. 7 shows, similar phenomena were observed upon exposure to a flow of CH_4 (0.25%) + O_2 (2.5%) + He, indicating that CH_4, though much more stable than *i*-C_4H_{10}, also reacts vigorously with NO_y complexes. Again, the intensity of the new bands increases with exposure time, but the band at 2955 cm^{-1} starts to decrease after 30 min.

Similar to the situation with Fe/MFI, the bands in the region of 1300 to 1700 cm^{-1} are attributed to the formation

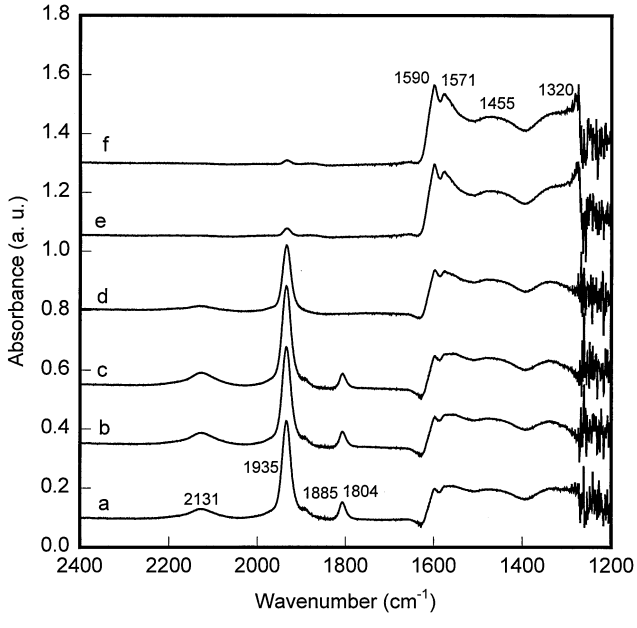

FIG. 5. FTIR spectra taken at 200°C of NO_y adsorbed Co/MFI-SUB under a flow of NO (0.5%) + O_2 (3%) + He for (a) 10 min, (b) 30 min, and (c) 60 min, followed by purge with a flow of O_2 (2.5%) + He for (d) 10 min, (e) 30 min, and (f) 60 min.

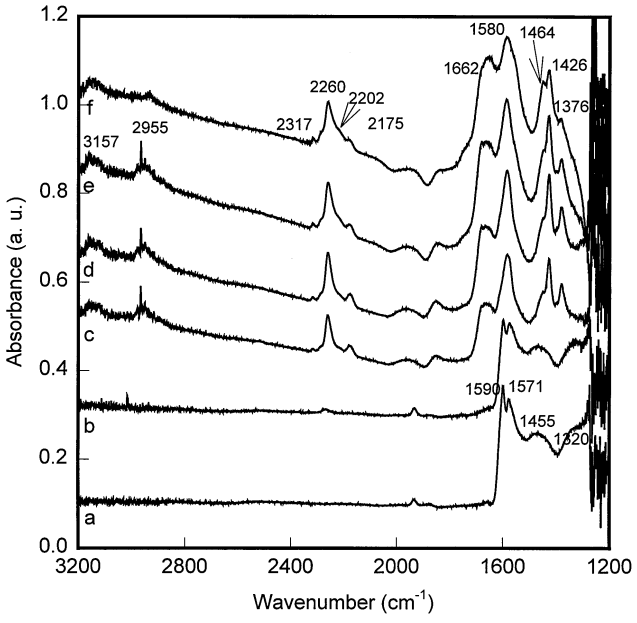

FIG. 6. FTIR spectra taken at 200°C of NO_y adsorbed Co/MFI-SUB and (a) purged with a flow of O_2 (2.5%) + He for 60 min; subsequently exposed to a flow of i-C_4H_{10} (0.25%) + O_2 (2.5%) + He for (b) 2 min, (c) 10 min, (d) 30 min, and (e) 60 min, (f) off i-C_4H_{10}, with a flow of O_2 (2.5%) + He for 60 min.

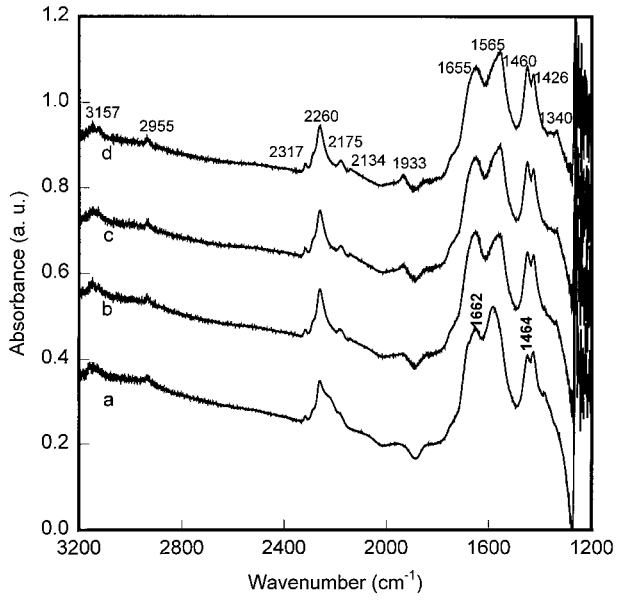

FIG. 8. FTIR spectra taken at 200°C after NO_y adsorbed Co/MFI-SUB exposed to a flow of i-C_4H_{10} (0.25%) + O_2 (2.5%) + He, (a) followed by purge with a flow of O_2 (2.5%) + He for 60 min; subsequently exposed to a flow of NO (0.5%) + O_2 (3%) + He for (b) 10 min, (c) 30 min, and (d) 60 min.

of some polymeric deposit on the catalysts (3). The precise assignment of the bands in the 2100- to 2300-cm^{-1} region is still unclear. A band at 2175 cm^{-1} is tentatively attributed to nitrile or isocyanate groups, Co^{2+}–CN (34) and Co^{2+}–NCO (35); the band at 2202 cm^{-1} is assigned to Co^{2+}–NCO (35, 36); and the band at 2260 cm^{-1} is assigned to Al^{3+}–NCO (34, 37). The 2955-cm^{-1} band in the C-H asymmetric vibration region can be ascribed to adsorbed CH_4 or i-C_4H_{10} (3, 36). This band is weaker for CH_4 than for i-C_4H_{10} and strongly decreases after a 60-min purge in an O_2 + He flow (curve f in Figs. 6 and Fig. 7). In contrast, the intensity of the bands at 1464 and 2202 cm^{-1} increases, while other bands retain their original intensity, indicating stability of the deposits and/or –NCO groups.

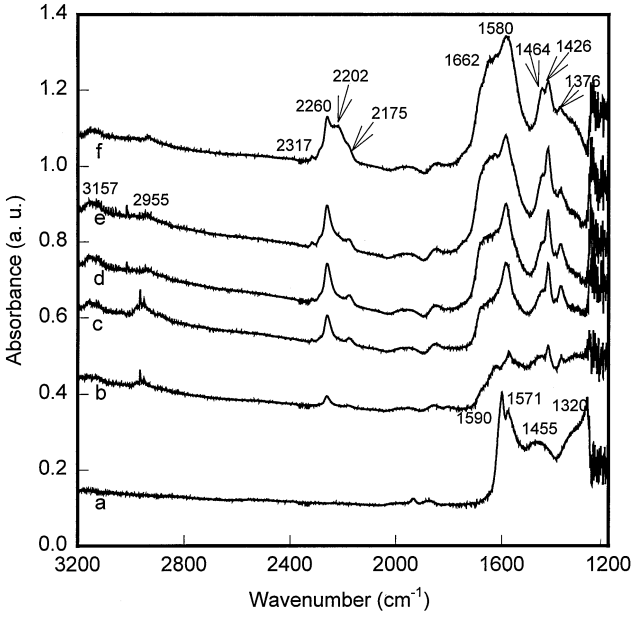

FIG. 7. FTIR spectra taken at 200°C of NO_y adsorbed Co/MFI-SUB and (a) purged with a flow of O_2 (2.5%) + He for 60 min; subsequently exposed to a flow of CH_4 (0.25%) + O_2 (2.5%) + He for (b) 2 min, (c) 10 min, (d) 30 min, and (e) 60 min, (f) off CH_4, with a flow of O_2 (2.5%) + He for 60 min.

Figure 8 shows the reactivity of gas phase NO + O_2 with the adsorbates formed by reaction of NO_y complexes with hydrocarbons. Curve a was recorded after reaction of NO_y with i-C_4H_{10}, followed by purging with O_2 + He at 200°C for 60 min. Upon re-exposure the catalyst to a flow of NO (0.5%) + O_2 (2.5%) + He, the band at 2202 cm^{-1} vanishes very rapidly, while the intensity of the 1464- and 1662-cm^{-1} bands increases. Bands appear at 1933 and 2134 cm^{-1}, indicating formation of mononitrosyl on the few Co^{2+} sites left unoccupied as well as formation of NO^+ on Brønsted acid sites in contact with the NO + O_2 + He atmosphere.

It has been reported that Fe/MFI-SUB (3) and Cu/MFI (32) show no activity when CH_4 is used as the reductant. Previous work in this lab shows that the nature of NO_y complexes on Cu/MFI differs from that on Co/MFI; the NO_y groups on Co/MFI are reactive to CH_4, while those on Cu/MFI are inert, thus leading to the absence of activity for NO_x reduction with CH_4 (32). Presumably, the same holds for Fe/MFI. To check this assumption, the reactivity toward

CH_4 of the NO_y complexes on Fe/MFI-SUB was examined at 200°C. As reported previously (3), two thermally stable NO_y bands at 1625 and 1570 cm^{-1} were formed, which have been ascribed to nitro and nitrate complexes, respectively. Then, this NO_y-covered Fe/MFI-SUB sample was exposed to a flow of CH_4 (0.25%) + O_2 (2.5%) + He. After 30 min, no obvious change in the intensity of the two bands was observed (results not shown). This is in contrast to the Co/MFI catalysts. We conclude though the NO_y groups of Fe/MFI-SUB are very reactive toward i-C_4H_{10} and other hydrocarbons, they are unreactive to CH_4.

3.4. *Mass Spectrometric Analysis of the Reaction Steps*

While FTIR results provide information on the adsorption complexes and their reactivity toward i-C_4H_{10} and CH_4, the gas phase products have been analyzed by mass spectrometry. As CO and $^{14}N_2$ have the same mass ($m/e = 28$) and CO_2 and $^{14}N_2O$ give the same signal ($m/e = 44$), we have used labeled ^{15}NO in these experiments. Very weak signals were obtained with CH_4 as the reductant; therefore, only results obtained with i-C_4H_{10} will be presented. We will show the data obtained with Co/MFI-SUB; those of Co/MFI-WIE are very similar.

The Co/MFI-SUB catalyst was first calcined in a UHP O_2 flow at 500°C for 1 h and then cooled to 200°C. The following experiments were carried out at this temperature. After evacuation for 30 min, the sample was exposed to a circulating gas mixture of 20 Torr ^{15}NO + 70 Torr O_2 + 10 Torr Ar for 1 h. As testified by TPD-MS and FTIR results, after this step, NO_y complexes were formed on the catalyst. After the system was evacuated for 30 min, a gas mixture of 20 Torr i-C_4H_{10} + 70 Torr O_2 + 10 Torr Ar was introduced into it and pumped to circulate through the catalyst. During gas circulation a small amount of $^{15}N_2$ and CO_2 was released, even less $^{15}N_2O$ was formed, and the amount of i-C_4H_{10} decreased (results not shown). This suggests that i-C_4H_{10} reacted with the NO_y complexes, mainly to form a deposit containing C, N, or O, perhaps –NCO groups. As shown in Figs. 6–8, i-C_4H_{10} and CH_4 react swiftly with the NO_y complexes to form –NCO bands, which react rapidly with gas phase NO + O_2.

After this step, the system was evacuated for 30 min and then a mixture of 20 Torr ^{15}NO + 70 Torr O_2 + 10 Torr Ar was introduced and circulated over the catalyst for ~1 h. The results are shown in Fig. 9. A large amount of $^{15}N_2$, CO_2, CO, and some $^{15}N_2O$ are formed. The amount of $^{15}N_2$ is much larger than that in the previous step when i-C_4H_{10} reacts with NO_y groups. Clearly, the interaction of NO + O_2 with the deposit is the main source of N_2.

To eliminate the possibility that a carbonaceous deposit merely acts as a reductant for impinging NO or NO_2, as proposed by some authors (38), we created a deposit by contacting a freshly calcined Co/MFI-SUB catalyst with a mixture of 20 Torr i-C_4H_{10} + 70 Torr O_2 + 10 Torr Ar for 1 h.

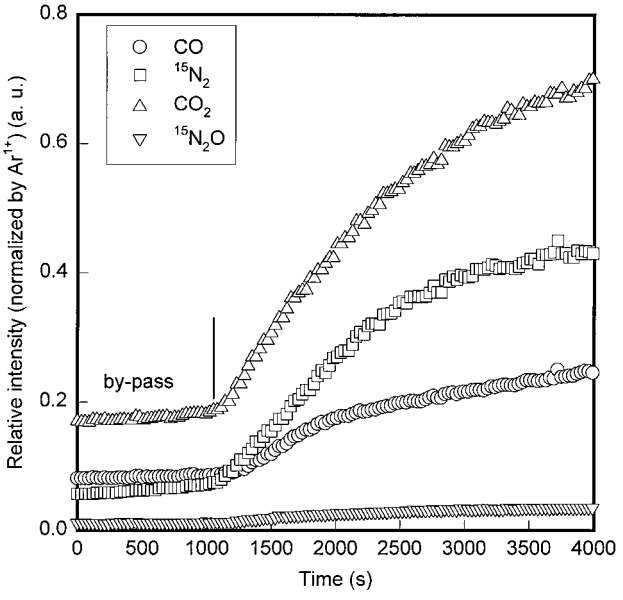

FIG. 9. Time dependence of the relative signal intensity upon circulating a mixture of 20 Torr ^{15}NO + 10 Torr Ar + 70 Torr O_2 over Co/MFI-SUB, on which a ^{15}N-containing deposit has been formed with i-C_4H_{10}.

After evacuation for 30 min, this sample was exposed to a circulating mixture of 20 Torr ^{15}NO + 70 Torr O_2 + 10 Torr Ar for 1 h. As shown in Fig. 10, much less $^{15}N_2$ was formed, with the amount being $\sim\frac{1}{3}$ of that in Fig. 9. However, the amounts of CO, CO_2, and $^{15}N_2O$ formed in this experiment were comparable to those shown in Fig. 9.

It thus follows that, for an efficient formation of N_2, the deposit has to be formed from the reaction between

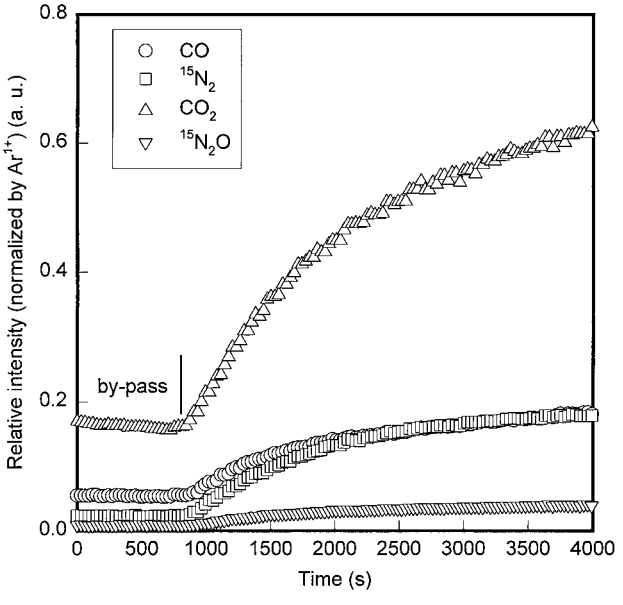

FIG. 10. Time dependence of the relative signal intensity upon circulating a mixture of 20 Torr ^{15}NO + 10 Torr Ar + 70 Torr O_2 over Co/MFI-SUB, on which a $C_xH_yO_z$ deposit has been formed directly with i-C_4H_{10}.

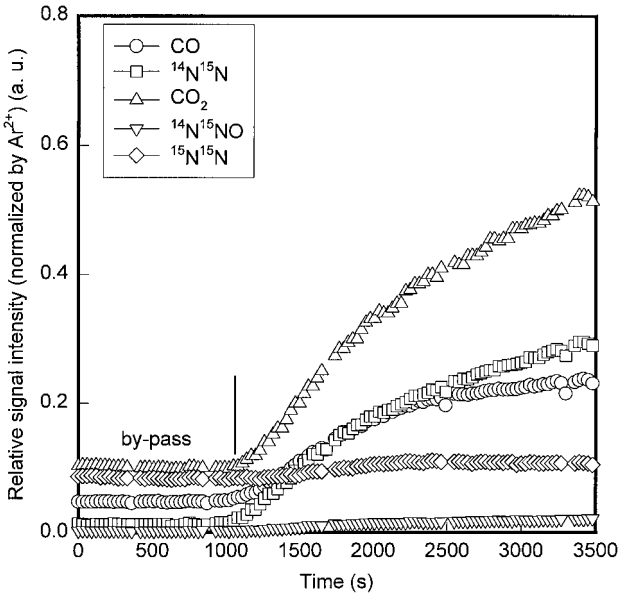

FIG. 11. Time dependence of the relative signal intensity upon circulating a mixture of 20 Torr $^{15}NO + 10$ Torr Ar + 70 Torr O_2 over Co/MFI-SUB, on which a ^{14}N-containing deposit has been formed with *i*-C_4H_{10}.

hydrocarbons and NO_y complexes. Similar to our previous work with Fe/MFI (3), an experiment using ^{15}N-labeled NO was carried out. First, a deposit was created on freshly calcined Co/MFI-SUB by the reaction of $^{14}NO_y$ complexes with *i*-C_4H_{10}. After evacuation of the gas, this deposit-laden sample was exposed to a circulating gas mixture of 20 Torr $^{15}NO + 70$ Torr $O_2 + 10$ Torr Ar for 1 h. The results are shown in Fig. 11. Clearly, the main N_2 product is the heteronuclear molecule $^{14}N^{15}N$. Only negligible amounts of $^{15}N_2$ and $^{14}N^{15}NO$ are formed. In addition, CO and CO_2 are produced. It follows that, in the reactions of $NO + O_2$ with the deposit formed by previous interaction of hydrocarbon with the NO_y complex on the catalyst, N_2 molecules are formed in which one N atom comes from the deposit and the other from the NO in the gas phase.

To clarify the effect of O_2 on the overall reaction, a ^{15}N labeled deposit was formed by reaction of *i*-C_4H_{10} with the $^{15}NO_y$ complexes on a freshly calcined Co/MFI-SUB catalyst, and this deposit-laden sample was exposed to a circulating gas mixture of 20 Torr $^{15}NO + 80$ Torr Ar (results not shown). In this case, much less $^{15}N_2$, CO, and CO_2 are formed than in the experiment of Fig. 9. Clearly, the O_2, present in the former but omitted in the latter experiment, plays an important role. The amounts of $^{15}N_2O$ were comparable in both runs.

3.5. CH_4 Exchange with D_2 over Partially Reduced Co/MFI-SUB

Our TPR data show that, with Co/MFI catalysts, the effective redox couple is probably $\boldsymbol{n}\mathbf{Co^{2+}/Co^0_n}$ (7, 8), whereas the $\mathbf{Fe^{3+}/Fe^{2+}}$ couple is active in Fe/MFI. To address the question of whether or not Co^0_n clusters activate the C–H bonds in CH_4, we used the CH_4 exchange with D_2 over a partially reduced Co/MFI-SUB catalyst as a probe for Co^0_n clusters. Our EPR results indicate that Co^0_n clusters are indeed formed when Co/MFI-SUB is reduced with H_2 at 300°C. As our previous results show near absence of Brønsted acid sites on this catalyst (7), any H/D exchange of methane has to be ascribed to Co metal sites.

As shown in Fig. 12a, the $m/e = 4$ (D_2) signal decreases with the time, while the $m/e = 3$ and $m/e = 2$ signals increase, showing the formation of (HD) and (H_2). Simultaneously, the $m/e = 16$ and 15 signals of CH_4 also decrease (results not shown), indicating that CH_4 is consumed. No CO ($m/e = 28$) or CO_2 ($m/e = 44$) is formed; this eliminates the possibility that CH_4 reacts with the residual oxygen impurities. These results confirm that CH_4 is mainly consumed by exchange with D_2. The formation of the exchange products is shown in Fig. 12b. The parent signals of CDH_3 ($m/e = 17$), CD_2H_2 ($m/e = 18$), CD_3H ($m/e = 19$), and CD_4 ($m/e = 20$) after subtraction of other possible fragments having the same m/e value also increase with the time. The relative concentrations of d_1, d_2, d_3, and d_4 differ from those reported in the literature (39, 40) for Co films. This could mean that some of the present signals are perturbed by the parent signals of H_2O ($m/e = 18$), HDO ($m/e = 19$), and D_2O ($m/e = 20$). However, it appears safe to ascribe the

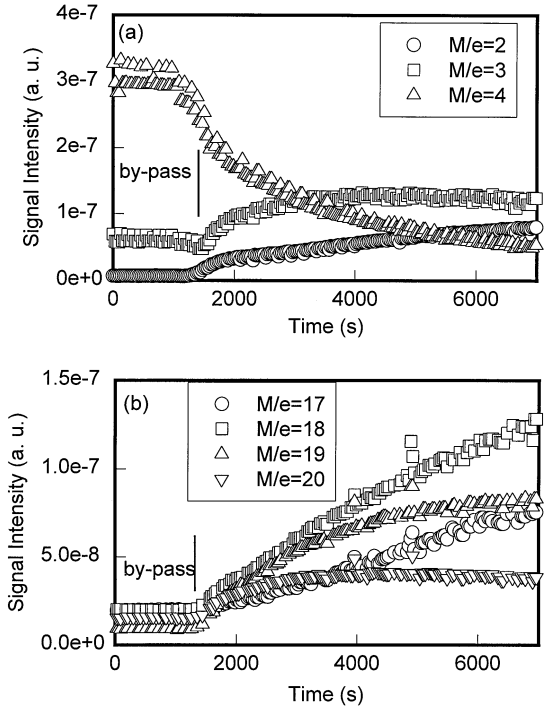

FIG. 12. Time dependence of the signal intensity upon circulating a mixture of 40 Torr $CH_4 + 40$ Torr D_2 over a partially reduced Co/MFI-SUB.

$m/e = 17$ signal to CH_3D because it is known that the OH^+ fragment ion of H_2O and HDO has an extremely low intensity (41). The formation of CDH_3 thus unambiguously shows that Co_n^0 sites exist in Co/MFI-SUB after reduction at 300°C.

4. DISCUSSION

Comparison of Fe/MFI and Co/MFI catalysts for the reduction of NO_x with hydrocarbons in a gas flow containing substantial concentrations of O_2 and H_2O reveals commonalities but also significant differences between both classes. For both types the performance depends strongly on the catalyst preparation method. For Fe/MFI a high metal loading is crucial and only catalysts with an Fe/Al ratio near unity, as achieved by the sublimation method, convert a large fraction of the NO_x in the feed to N_2. Co/MFI catalysts are less demanding in this respect. Catalysts with Co/Al ratios below 0.5 achieve N_2 yields near 100%, but the temperature required for this performance is higher than that for the most active catalysts, which have a Co/Al ratio near unity and thus use extralattice oxygen to compensate part of the positive charge of the Co ions. All Co/MFI catalysts are capable of reducing NO_x with methane to some extent, whereas the Fe/MFI catalysts lack this ability.

As to the mechanism of NO_x reduction, a multistep model is emerging that shows many commonalities among Fe and Co catalysts. The opening act is the interaction of $NO + O_2$ with the catalyst, resulting in the formation of an "NO_y" adsorption complex. Though such adsorbates are also formed on the metal-free zeolite, they are strongly stabilized by interaction with the transition metal ion. Roughly speaking, they can be considered nitrate ions. These NO_y groups interact chemically with an impinging hydrocarbon, such as i-C_4H_{10}. Though little N_2 is formed in this step, a new adsorbed intermediate is formed containing C, N, and O atoms. In a subsequent step this intermediate reacts with $NO + O_2$ or NO_2; in this crucial step N_2 molecules are formed with one N atom from the impinging NO_2 and the other is from the surface intermediate. This mechanism appears valid for both Fe/MFI (3) and Co/MFI catalysts.

A matter of discussion is the precise nature of the NO_y groups and to what extent their spectroscopic signature differs for Fe/MFI and Co/MFI. With Co/MFI of low Co/Al ratio Adelman *et al.* found two NO_y bands at 1526 and 1310 cm^{-1}, respectively (32). They ascribed the former band to a nitrito group ($Co^{2+}ONO$) and the latter to the vibration of nitrito, nitro ($Co^{2+}NO_2$), and chelating nitro ($Co^{2+}O_2N$) groups. In the present work with Co/MFI of Co/Al ratios near unity, no 1526-cm^{-1} band is observed, while one does appear at 1320 cm^{-1}. Hadjiivanov *et al.* found four bands at 1536, 1578, 1600, and 1643 cm^{-1} (30) and assigned them to different surface nitrates. The bands at 1578 and 1600 cm^{-1} are similar to those at 1571 and 1590 cm^{-1} found in our experiments. It thus appears that the NO_y complex on Co/MFI may be visualized as nitrate, nitrito, and nitro groups attached to Co ions. On FeMFI the NO_y groups are also believed to consist of nitrate ions and nitro groups, both interacting with Fe ions (3).

The rates by which the NO_y groups and gaseous NO_2 are formed are different for Co/MFI and Fe/MFI. Previous work showed that Fe/MFI-SUB is very active, catalyzing NO_2 formation even at ambient temperature. This activity has been ascribed to the presence of the bridging oxygen in $[HO–Fe–O–Fe–OH]^{2+}$ (3, 19). The present work shows that passing of NO (0.7%) + O_2 (6%) through a bed of Co/MFI-WIE or Co/MFI-SUB produces much less NO_2 than was found over Fe/MFI-SUB under the same conditions. This may be the main reason why Fe/MFI-SUB below 350°C displays a higher N_2 yield than the Co/MFI catalysts. It thus appears that Fe/MFI-SUB is more active, but Co/MFI catalysts are more selective because they are less active for the combustion of i-C_4H_{10}. Among the two Co/MFI catalysts, the overexchanged Co/MFI-SUB is obviously the most active one. $NO + O_2$ adsorption results show that NO_2 saturation is reached more rapidly over it than over Co/MFI-WIE. We doubt that isolated Co^{2+} ions are able to catalyze NO oxidation to NO_2. It is more probable that small amounts of Co_3O_4 or residual Brønsted acid sites (42) in Co/MFI-WIE are responsible for the slow NO_2 formation that is observed. Our previous TPR results showed that with Co/MFI-WIE only a small reduction peak was detected at 705°C, whereas with Co/MFI-SUB pronounced TPR peaks were observed at 220 and 385°C (7). The peak at 220°C has been attributed to multinuclear Co oxo ions and the 385°C peak to Co_3O_4 clusters. Integration of the TPD profiles for $m/e = 30$ in Fig. 3 shows that the ratio of the peak areas is much larger for Co/MFI-SUB than for Co/MFI-WIE. This indicates that more NO_y is formed on Co/MFI-SUB. It is likely that the Co oxo ions in Co/MFI-SUB are responsible for the higher efficiency of this preparation to produce NO_y and thus to reduce NO_x.

To form a nitrate ion from an NO molecule, two oxygen atoms and one electron have to be added. The simplest way to visualize this is to assume that the NO molecule reacts with a superoxide ion (43, 44):

$$NO + O_2^- = NO_3^-. \qquad [4]$$

For a metal-free catalyst such as H-MFI, the parent cation will be a nitrosonium ion, NO^+. The ion pair $NO^+NO_3^-$ can decompose into two NO_2 molecules. Unpublished results in our lab are consistent with this chemistry. On metal-containing zeolites, Fe/MFI or Co/MFI, the nitrate ions, nitro, and nitrosonium groups will be stabilized by interaction with the metal ion. Formation of a superoxide ion upon exposure of Co/MFI, with Co in its low-spin state, has

been proven by EPR at 77 K (45):

$$Co^{2+} + O_2 = Co^{3+} \cdots O_2^- . \quad [5]$$

The O_2^- ion is so close to the Co nucleus that interaction with the nuclear spin of the latter results in a super-hyperfine splitting in eight states.

The results in Fig. 4 are of possible relevance to the oxidation of NO_{ads} by O_2. In the absence of O_2, NO is mainly adsorbed on Co/MFI as Co^{2+}–NO and, to a lesser extent, $Co^{2+}(NO)_2$ complexes, in accordance with the NO-TPD results in Fig. 2. Upon the samples being purged with a UHP He flow, the IR intensity of the bands of the mononitrosyl and dinitrosyl groups decreases slowly. In contrast, upon the samples being purged with an O_2 + He gas mixture, the original absorption bands all but vanish within 40 min; formation of NO_y groups is detected in the region of 1200–1600 cm^{-1}. When the catalyst was exposed to a mixture of NO + O_2, very strong NO_y bands were observed in addition to the mononitrosyl and dinitrosyl bands. It follows that adsorbed NO groups are converted with O_2 to NO_y complexes; the extent of this reaction is large if the consumed NO_{ads} is replaced from the gas phase. As the superoxide ion will have a short life at this temperature, it stands to reason that the formation of nitrate ions will be most efficient when NO and O_2 molecules hit the surface in short succession, i.e., from a mixture of both gases.

The signal of the O_2^- ion has also been observed with overexchanged Cu/MFI (46) and Fe/MFI (19) catalysts. It thus appears probable that the superoxide ion plays a key role in the formation of the NO_y groups (13) on Fe/MFI-SUB catalysts and thus also in the formation of NO_2.

The IR results in Fig. 7 show that the NO_y groups (bands at 1590 and 1320 cm^{-1}) of Co/MFI react rather vigorously with CH_4, whereas the nitro/nitrate complexes of Fe/MFI-SUB do not react with CH_4. Apparently, the NO_y groups in both catalysts differ chemically.

After the samples were purged with an O_2 + He flow and exposed to an NO + O_2 + He flow, the bands in the region of 1600–2000 cm^{-1} do not decrease, while bands at 1464 and 1662 cm^{-1} increase. However, a band at 2202 cm^{-1}, which is assigned to –NCO, disappears rapidly. This suggests that isocyanate in Co/MFI could act as an important intermediate, as has been suggested by other authors (36, 47, 48). Our mass spectrometric results show that a large amount of N_2 is produced, with most of it having one N atom from the deposit and another from the gas phase NO_2. Only little N_2O is formed, and it is not a likely intermediate of the NO_x SCR reaction.

TPR results show that, in Fe/MFI, the redox couple Fe^{3+}/Fe^{2+} is operating (1) and in Cu/MFI it is Cu^{2+}/Cu^{+} (49). In contrast, Co^{2+} reduction in Co/MFI gives Co^0 in one step (7), indicating the redox couple Co^{2+}/Co^0. Likewise, Pd^{2+} in Pd/MFI (50–52) is reduced to Pd^0 in one step. It is interesting that among these four catalysts those that are able to reduce NO_x with methane are also those that use the zerovalent state of the metal in their redox couple. Admittedly, it seems rather difficult to imagine that Co_n^0 clusters can exist under the conditions of NO_x reduction, in particular with catalysts that were produced by wet ion exchange and thus have initially isolated Co^{2+} ions that are difficult to reduce. Still, the possibility that methane is activated on Co_n^0 clusters cannot be entirely dismissed since isolated ions in zeolites are known to agglomerate by hydrolysis to oxo ions that are easily reduced. At present, most authors assume that over Co/MFI methane is activated on adsorbed NO_y complexes (25, 53, 54) and over Pd/HMFI on bare Pd ions (42, 55). In that view the cause for the qualitative differences between two groups of chemically similar elements is less obvious than if a role of the metallic state is assumed in methane activation.

5. CONCLUSIONS

The reaction mechanism of NO_x reduction with isobutane appears to be similar over Fe/MFI and Co/MFI, although Fe/MFI is more active and Co/MFI is more selective. In both cases adsorbed NO reacts with O_2 and is converted to "NO_y" groups; however, this conversion is faster with Fe/MFI. One can speculate that O_2 is adsorbed as a superoxide ion, O_2^-, which reacts with NO to a nitrate ion, NO_3^-. As part of the NO is adsorbed as NO^+, the ion pair NO^+ NO_3^- can decompose to $2NO_2$ molecules. Both the NO_3^- ion and the NO_2 molecules can form stable complexes with Co^{2+} and Fe^{3+} ions. They give rise to the IR signals, conventionally ascribed to the NO_y adsorbate. On Co^{2+} part of NO_2 may be attached as an ONO^- ion. Interaction of the adsorbate with isobutane at 200°C leads to the formation of a deposit, apparently exposing nitrile and isocyanate groups. Subsequent interaction with gaseous NO + O_2 leads to the formation of N_2 with one atom from the gaseous NO and the other from the deposit.

Co/MFI catalyzes the reduction of NO_x with methane, while Fe/MFI does not. Either the NO_y groups ligated to Co or Fe are chemically different or the high activity of Co/MFI toward methane is due to Co_n^0 clusters. Their formation is suggested by the TPR data; in mildly reduced catalysts they have been identified by their propensity to catalyze the H/D exchange between CH_4 and D_2. In contrast, no Fe_n^0 clusters exist in Fe/MFI under comparable reduction conditions.

ACKNOWLEDGMENTS

This work was supported by the EMSI program of the National Science Foundation and the U.S. Department of Energy Office of Science (CHE-9810378) at the Northwestern University Institute for Environmental Catalysis. Financial aid from the Director of the Chemistry Division, Basic Energy Sciences, U.S. Department of Energy, Grant DE-FGO2-87ER13654, is gratefully acknowledged.

REFERENCES

1. Chen, H.-Y., and Sachtler, W. M. H., *Catal. Today* **42**, 73 (1998).
2. Chen, H.-Y., Wang, X., and Sachtler, W. M. H., *Appl. Catal. A* **194**, 195 (2000).
3. Chen, H.-Y., Voskoboinikov, T., and Sachtler, W. M. H., *J. Catal.* **180**, 171 (1998).
4. Voskoboinikov, T., Chen, H.-Y., and Sachtler, W. M. H., *Appl. Catal.* **19**, 279 (1998).
5. Chen, H.-Y., Voskoboinikov, T., and Sachtler, W. M. H., *J. Catal.* **186**, 91 (1999).
6. Chen, H.-Y., and Sachtler, W. M. H., *Catal. Lett.* **50**, 125 (1998).
7. Wang, X., Chen, H.-Y., and Sachtler, W. M. H., *Appl. Catal. B* **26**, L227 (2000).
8. Wang, X., Chen, H.-Y., and Sachtler, W. M. H., *Appl. Catal. B*, in press.
9. Chen, H.-Y., Voskoboinikov, T., and Sachtler, W. M. H., *Catal. Today* **54**, 483 (1999).
10. Voskoboinikov, T., Chen, H.-Y., and Sachtler, W. M. H., *J. Mol. Catal. A* **155**, 155 (2000).
11. Long, R. Q., and Yang, R. T., *J. Am. Chem. Soc.* **121**, 5595 (1998).
12. Kögel, M., Mönnig, M., Schwieger, W., Tissler, A., and Turek, T., *J. Catal.* **182**, 470 (1999).
13. Lobree, L. J., Hwang, I.-C., Reimer, J. A., and Bell, A. T., *Catal. Lett.* **63**, 233 (1999).
14. Lobree, L. J., Hwang, I.-C., Reimer, J. A., and Bell, A. T., *J. Catal.* **186**, 242 (1999).
15. Chen, H.-Y., Wang, X., and Sachtler, W. M. H., *Phys. Chem. Chem. Phys.* **2**, 3083 (2000).
16. Giles, R., Richard, Cant, N. W., Kögel, M., Turek, T., and Trimm, D., *Appl. Catal. B* **25**, L75 (2000).
17. Marturano, P., Drozdová, L., Kogelbauer, A., and Prins, R., *J. Catal.* **192**, 236 (2000).
18. El-Malki, El-M., van Santen, R. A., and Sachtler, W. M. H., *Microporous Mesoporous Mater.* **35**, 235 (2000).
19. Chen, H.-Y., El-Malki, El-M., Wang, X., van Santen, R. A., and Sachtler, W. M. H., *J. Mol. Catal.*, in press.
20. Li, Y., Battavio, P. J., and Armor, J. N., *J. Catal.* **142**, 561 (1993).
21. Li, Y., and Armor, J. N., *Appl. Catal. B* **1**, L31 (1992).
22. Li, Y., and Armor, J. N., *Appl. Catal. B* **2**, 239 (1993).
23. Dean, J. A., "Analytical Chemistry Handbook." McGraw-Hill, New York, 1995.
24. Hadjiivanov, K., Saussey, J., Freysz, J. L., and Lavalley, J. C., *Catal. Lett.* **52**, 103 (1998).
25. Li, Y., Slager, T. L., and Armor, J. N., *J. Catal.* **150**, 388 (1994).
26. Iwamoto, M., and Hoshino, Y., *Chem. Lett.* 729 (1995).
27. Zhu, C. Y., Lee, C. W., and Chong, P. J., *Zeolites* **17**, 483 (1996).
28. Campa, M. C., De Rossi, Ferraris, S., G., and Indovina, V., *Appl. Catal. B* **8**, 315 (1996).
29. Aylor, A. W., Lobree, L. J., Reimer, J. A., and Bell, A. T., *Stud. Surf. Sci. Catal* **101**, 661 (1996).
30. Hadjiivanov, K., Tsyntsarski, B., and Nikolova, T., *Phys. Chem. Chem. Phys.* **1**, 4521 (1999).
31. Pinaeva, L. G., Sadovskaya, E. M., Suknev, A. P., Goncharov, V. B., Sadykov, V. A., Balzhinimaev, B. S., Decamp, T., and Mirodatos, C., *Chem. Eng. Sci.* **54**, 4327 (1999).
32. Adelman, B. J., Beutel, T., Lei, G. D., and Sachtler, W. M. H., *J. Catal.* **158**, 327 (1996).
33. Campa, M. C., Pietrogiacomi, D., Tuti, S., Ferraris, G., and Indovina, V., *Appl. Catal. B* **18**, 151 (1998).
34. Lobree, L. J., Aylor, A. W., Reimer, J. A., and Bell, A. T., *J. Catal.* **169**, 188 (1997).
35. Satsuma, A., Cowan, A. D., Cant, N. W., and Trimm, D. L., *J. Catal.* **180**, 1 (1998).
36. Goryashenko, S. S., Park, Y. K., Kim, D. S., and Park, S.-E., *Res. Chem. Intermed.* **24**, 933 (1998).
37. Solymosi, F., and Bansagi, T., *J. Catal.* **156**, 75 (1995).
38. Walker, A. P., *Catal. Today* **26**, 107 (1995).
39. Kemball, C., "Advance in Catalysis." Academic Press, New York, 1959.
40. Thompson, S. O., Turkevich, J., and Irsa, A. P., *J. Am. Chem. Soc.* **73**, 5213 (1951).
41. Stenhagen, E., Abrahamsson, S., and Mclafferty, F. W., "Atlas of Mass Spectral Data." Interscience, New York, 1969.
42. Misono, M., *Cattech* **4**, 183 (1998).
43. Radi, R., Beckman, J. S., Bush, K. M., and Freeman, B. A., *J. Biol. Chem.* **266**, 4244 (1991).
44. Plumb, R. C., and Edwards, J. O., *J. Phys. Chem.* **96**, 3245 (1992).
45. El-Malki, El-M., Werst, D., Doan, P. E., van Santen, R. A., and Sachtler, W. M. H., *J. Phys. Chem.*, in press.
46. Sárkány, J., and Sachtler, W. M. H., *Stud. Surf. Sci. Catal.* **94**, 649 (1995).
47. Hwang, I. C., Kim, D. H., and Woo, S. I., *Catal. Today* **44**, 47 (1998).
48. Hadjiivanov, K., Knözinger, H., Tsyntsarski, B., and Dimitrov, L., *Catal. Lett.* **62**, 35 (1999).
49. Beutel, T., Sárkány, J., Lei, J. G., Yan, J. Y., and Sachtler, W. M. H., *J. Phys. Chem.* **100**, 845 (1996).
50. Nishizaka, Y., and Misono, M., *Chem. Lett.* 1295 (1993).
51. Ogura, M., Hayashi, M., Kage, S., Matsukata, M., and Kikuchi, E., *Appl. Catal. B* **23**, 247 (1999).
52. Lobree, L. J. A., Aylor, W., Reimer, J. A., and Bell, A. T., *J. Catal.* **181**, 189 (1999).
53. Cowan, A. D., Dümpelmann, R., and Cant, N. W., *J. Catal.* **151**, 356 (1995).
54. Halasz, I., Brener, A., and Ng, K. Y. S., *Catal. Lett.* **34**, 151 (1995).
55. Nishizaka, Y., and Misono, M., *Chem. Lett.* 2237 (1994).